EPTT 2024
Escola de Primavera de Transição e Turbulência

ABCM
Associação Brasileira de Engenharia e Ciências Mecânicas

EPTT-2024-0028
STABILITY ANALYSIS OF OLDROYD-B AND GIESEKUS FLUIDS JET FLOW: LST AND DNS

Rafael de Lima Sterza
Leandro Franco de Souza
Universidade de São Paulo, Instituto de Ciências Matemáticas e de Computação, São Carlos - SP, Brasil
rafael.sterza@usp.br; lefraso@icmc.usp.br

Analice Costacurta Brandi
Universidade Estadual Paulista, Faculdade de Ciências e Tecnologia, Presidente Prudente - SP, Brasil
analice.brandi@unesp.br

Marcio Teixeira de Mendonça
Instituto de Aeronáutica e Espaço, Cachoeira Paulista - SP, Brasil
marcio_tm@yahoo.com

Abstract. *Using approaches from Linear Stability Theory and Direct Numerical Simulation, this article compares the stability properties of jet flows utilizing Oldroyd-B and Giesekus fluids. The purpose of the study is to clarify how viscoelasticity affects fluid jet stability behavior, which is a feature of many industrial and natural processes. Additionally, the stability properties of jet flows involving Oldroyd-B and Giesekus fluids will be compared in this study. The results section presents the stability characteristics obtained through the LST and DNS approaches for different flow parameters and rheological properties of the fluids. By using the two fluid models, the comparison highlights the disparities in their stability behavior and clarifies the function of viscoelasticity in jet flow stability.*

Keywords: *Jet flow, Oldroyd-B fluid, Giesekus fluid, Linear Stability Theory, Direct Numerical Simulation*

1. INTRODUCTION

Laminar-turbulent transition is the process of altering laminar flow to take it to the turbulent regime. To predict these changes, hydrodynamic stability analysis is carried out. Instabilities in base flow are typically linked to the change from laminar to turbulent flow. One way to comprehend the instabilities that cause laminar flow to change into turbulent flow is to apply Linear Stability Theory (LST). It is based on the linearized analysis of the Navier-Stokes equations around a state of laminar equilibrium. This analysis allows the identification of exponentially growing modes of instability, i.e., regions where laminar flow is vulnerable to disturbances that may cause the flow to become turbulent. On the other hand, Direct Numerical Simulation (DNS) is a sophisticated computational tool that does not rely on simplifying assumptions and is used to directly investigate turbulent flow behavior.

Non-Newtonian fluid flows, particularly in confined geometries, have garnered significant attention in the literature. Studies have shown that parameters such as β and Weissenberg (Wi) parameters greatly influence the stability of planar Poiseuille flow for fluids like Oldroyd-B and Giesekus (Brandi *et al.*, 2019; Furlan *et al.*, 2018; Brandi *et al.*, 2017). Researchers have explored both modal and non-modal stability of various non-Newtonian fluids, shedding light on their behavior in channel and jet flows (Zhang *et al.*, 2013).

The investigation of non-Newtonian fluid jet flows holds substantial importance for industrial applications such as polymer processing and drag reduction. The work of Rallison and Hinch (1995), who examined the submerged elastic jet characterized by a parabolic profile flow for high Reynolds numbers, can be considered one of the earliest studies in non-Newtonian jet flow. They discovered that although the varicose mode is only partially stabilized, the sinuous mode is fully stabilized by strong elasticity. The Oldroyd-B constitutive equation was used to model the viscoelastic flow in his linear stability analysis. As the elastic effect increases, the flow becomes more stable but is not completely stable. Zhang (2012) studied the viscoelastic jet problem, where the constitutive equation was derived using the Oldroyd-B model. The results of this study's modal stability analysis in polymeric jets showed that, for small Reynolds numbers, the elastic effect

not only influenced hydrodynamic instability by raising the critical Reynolds number but also gave rise to a new instability mechanism known as elastic instability.

Many investigators are employing diverse methodologies to carry out investigations concerning jet flows and stability analysis. For example, using viscoelastic FENE-P fluids, Guimarães *et al.* (2020) carried out direct numerical simulations of turbulent planar jets made up of diluted polymer solutions. Comparing the viscoelastic jets to the Newtonian reference jet, they found that the latter had slower spreading and decay rates. Furthermore, it was found that viscoelastic jets had Reynolds stresses that were smaller than those of the reference Newtonian jet. Later, Guimarães *et al.* (2023) used viscoelastic FENE-P fluids at high Reynolds numbers to conduct direct numerical simulations to study the spatial evolution of submerged jets. According to the findings, shorter waves in the linear regime destabilized first, and as the Weissenberg number rose, this effect spread to longer waves, increasing instability in the majority of modes.

This paper aims to analyze the stability dynamics of jet flows using both Linear Stability Theory and Direct Numerical Simulation, focusing on two-dimensional, planar, incompressible, submerged jets that discharge from a nozzle into a medium that contains the same fluid as the jet. Verifying the impact of the viscoelastic extra-tension tensor model on the stability patterns displayed by these flows is the primary goal. The study clarifies the behavior of convective stability in these flows by comparing and contrasting the stability properties of the Oldroyd-B and Giesekus models. By comparing the results obtained from these two approaches, we seek to clarify the impact of viscoelasticity on the stability patterns exhibited by these flows. Previous studies have provided valuable insights into the stability properties of individual models (Sterza *et al.*, 2022, 2023a,b); however, this work aims to verify and extend these findings through a comprehensive comparative analysis.

In the results section, the stability characteristics are shown using the LST and DNS methods. These analyses provide a brief comparison between the Oldroyd-B and Giesekus models' instability regions by using a temporal analysis. An excellent correspondence between the results was verified in the comparison between the two stability analysis approaches (LST and DNS), which is the main verification.

2. MATHEMATICAL FORMULATION

Considering that the flow is non-Newtonian, two-dimensional, incompressible, and isothermal, the dimensionless forms of the mass and momentum balance equations are given by:

$$\nabla \cdot \mathbf{u} = 0, \tag{1}$$

$$\frac{\partial \mathbf{u}}{\partial t} + \nabla \cdot (\mathbf{u} \otimes \mathbf{u}) = -\nabla p + \frac{\beta}{Re}\nabla^2 \mathbf{u} + \nabla \cdot \mathbf{T}, \tag{2}$$

where $\mathbf{u}$ denotes the velocity field, t is the time, p is the pressure, β is the dimensionless coefficient of the solvent viscosity, Re is the Reynolds number and $\mathbf{T}$ is the extra-stress tensor. Constitutive equations that allow for the study of viscoelastic fluids model the stress tensor. This paper examined the Oldroyd-B and Giesekus models, which is given by

$$\mathbf{T} + Wi\overset{\nabla}{\mathbf{T}} + \alpha_G \frac{WiRe}{1-\beta}(\mathbf{T}\cdot\mathbf{T}) = \frac{(1-\beta)}{Re}\left(\nabla\mathbf{u} + (\nabla\mathbf{u})^T\right), \tag{3}$$

where Wi is the Weissenberg number, $\overset{\nabla}{\mathbf{T}}$ is the upper-convected derivative of $\mathbf{T}$, α_G is the so-called mobility parameter $(0 \leq \alpha_G \leq 1)$. The constitutive equation returns the Oldroyd-B model if $\alpha_G = 0$.

The streamwise and normal directions are represented by the variables x and y in our study of viscoelastic plane jet flow. It is assumed that the laminar base flow is parallel. The streamwise velocity of the jet base flow was proposed by Michalke (1971), and the non-Newtonian extra-stress tensor components of the base flow (for Oldroyd-B model, when $\alpha_G = 0$) are given by

$$U(y) = \frac{1}{2}\left[1 + \tanh\frac{R}{4\theta}\left(\frac{R}{y} - \frac{y}{R}\right)\right], \quad T_b^{yy} = 0, \qquad T_b^{xy} = \frac{(1-\beta)}{Re}\frac{dU}{dy} \qquad \text{and} \qquad T_b^{xx} = 2WiT_b^{xy}\frac{dU}{dy}, \tag{4}$$

where R denotes the jet half-width and θ the momentum boundary layer thickness.

For $\alpha_G \neq 0$, Eqs. (4) do not describe the solution of laminar flow, and it is not possible to directly determine each component of the tensors. Given this, with the fixed velocity profile $U(y)$ provided in Eq. (4), the following assumptions are considered: invariance in the x direction, and $v = 0$. These assumptions are applied to the transport equations for velocity and non-Newtonian tensors. In the resulting equations, the fourth-order Runge-Kutta method is applied for temporal advancement so that convergence to the base flow is ensured when the temporal derivatives are zero, as the base flow is considered stationary.

2.1 Linear Stability Theory

The behavior of a flow in response to an infinitesimal amplitude disturbance is analyzed by the linear stability theory. The flow is divided into two parts: a disturbed flow and a base flow, which is thought to be parallel and stationary. The disturbances are represented as normal modes by

$$\phi(x,y,t) = \overline{\phi}(y)e^{i(\alpha x-\omega t)}, \tag{5}$$

where $\overline{\phi}$ represents the magnitude and phase of the disturbances, $i=\sqrt{-1}$, $\alpha=\alpha_r$ is the wave number in the x direction and $\omega=\omega_r+i\omega_i$ represents the angular frequency and the temporal growth rate. Substituting the normal mode solution (5) into the disturbance Navier-Stokes and non-Newtonian extra-stress tensor equations, omitting the superscript from the notation we have

$$i\alpha u + \frac{dv}{dy} = 0, \tag{6}$$

$$-i\omega u + i\alpha u U + v\frac{dU}{dy} = -i\alpha p + \frac{\beta}{Re}\left[(i\alpha)^2 u + \frac{d^2u}{dy^2}\right] + i\alpha T^{xx} + \frac{dT^{xy}}{dy}, \tag{7}$$

$$-i\omega v + i\alpha v U = -\frac{dp}{dy} + \frac{\beta}{Re}\left[(i\alpha)^2 v + \frac{d^2v}{dy^2}\right] + i\alpha T^{xy} + \frac{dT^{yy}}{dy}, \tag{8}$$

$$\begin{aligned} T^{yy}\left(1-i(\omega-\alpha U)Wi\right) \;+\; & Wi\left(\frac{dT_b^{yy}}{dy}v - 2i\alpha v T_b^{xy} - 2\frac{dv}{dy}T_b^{yy}\right) + \frac{2\alpha_G Wi Re}{1-\beta}(T_b^{xy}T^{xy} + T_b^{yy}T^{yy}) = \\ = \; & \frac{2\,(1-\beta)}{Re}\frac{dv}{dy}, \end{aligned} \tag{9}$$

$$\begin{aligned} T^{xy}\left(1-i(\omega-\alpha U)Wi\right) \;+\; & Wi\left(v\frac{dT_b^{xy}}{dy} - i\alpha v T_b^{xx} - \frac{dU}{dy}T^{yy} - \frac{i}{\alpha}\frac{d^2v}{dy^2}T_b^{yy}\right) + \\ + \; & \frac{2\alpha_G Wi Re}{1-\beta}\left[T^{xy}(T_b^{xx}+T_b^{yy}) + T_b^{xy}(T^{xx}+T^{yy})\right] = \frac{(1-\beta)}{Re}\left(i\alpha v + \frac{i}{\alpha}\frac{d^2v}{dy^2}\right), \end{aligned} \tag{10}$$

$$\begin{aligned} T^{xx}\left(1-i(\omega-\alpha U)Wi\right) \;+\; & Wi\left(v\frac{dT_b^{xx}}{dy} + 2T_b^{xx}\frac{dv}{dy} - 2T_b^{xy}\frac{i}{\alpha}\frac{d^2v}{dy^2} - 2T^{xy}\frac{dU}{dy}\right) + \\ + \; & \frac{2\alpha_G Wi Re}{1-\beta}(T_b^{xx}T^{xx} + T_b^{xy}T^{xy}) = -\frac{2\,(1-\beta)}{Re}\frac{dv}{dy}. \end{aligned} \tag{11}$$

The boundary conditions for a two-dimensional plane jet with constant properties and no body forces are as follows (Kundu and Cohen, 2010),

$$\begin{aligned} u = v &= 0, \quad \text{for} \quad y \to \pm\infty, \\ v &= 0, \quad \text{for} \quad y = 0, \quad \text{(varicose mode)}, \\ p &= 0, \quad \text{for} \quad y = 0, \quad \text{(sinuous mode)}. \end{aligned}$$

2.2 Direct Numerical Simulation

Without any simplifications, Direct Numerical Simulation (DNS) solves the Navier-Stokes equations directly. Vorticity, or ω_z, is a basic concept in DNS that describes the local rotational motion of fluid particles mathematically. DNS decomposes the Navier-Stokes equations into vorticity equations by using the velocity-vorticity formulation. Thus, the two-dimensional vorticity's constituent parts are defined by

$$\omega_z = \frac{\partial u}{\partial y} - \frac{\partial v}{\partial x}. \tag{12}$$

We derive a new system of equations by algebraically modifying the governing equations and using the definition of vorticity.

$$\frac{\partial u}{\partial x} + \frac{\partial v}{\partial y} = 0, \tag{13}$$

$$\frac{\partial^2 v}{\partial x^2} + \frac{\partial^2 v}{\partial y^2} = -\frac{\partial \omega_z}{\partial x}, \tag{14}$$

$$\frac{\partial \omega_z}{\partial t} + \frac{\partial (u\omega_z)}{\partial x} + \frac{\partial (v\omega_z)}{\partial y} = \frac{\beta}{Re}\left[\frac{\partial^2 \omega_z}{\partial x^2} + \frac{\partial^2 \omega_z}{\partial y^2}\right] - \frac{\partial^2 T^{xy}}{\partial x^2} - \frac{\partial^2 T^{yy}}{\partial x \partial y} + \frac{\partial^2 T^{xx}}{\partial y \partial x} + \frac{\partial^2 T^{xy}}{\partial y^2}. \tag{15}$$

In addition to the equations above, one must consider the equations of non-Newtonian tensors (3) in two-dimensional Cartesian coordinates.

3. NUMERICAL FORMULATION

3.1 Stability Analysis

When combined with its boundary conditions, matrix stability analysis offers a method for determining a system's stability characteristics. In other words, the matrices L and F are obtained by writing equations (6) to (11) in matrix form,

$$L[u \quad v \quad p \quad T^{xx} \quad T^{yy} \quad T^{xy}]^\intercal = \omega F[u \quad v \quad p \quad T^{xx} \quad T^{yy} \quad T^{xy}]^\intercal. \tag{16}$$

Equation (16) represents the eigenvalue problem of Linear Stability Theory through temporal analysis, where ω is complex, while α is a real number. If $\omega_i > 0$, then the flow is unstable.

Chebyshev points and Chebyshev differentiation matrices were used to calculate the derivatives. It is important to note that the matrix stability analysis is used for a velocity profile with an infinitely long y-directed hyperbolic tangent function that shows steep gradients close to the jet. Chebyshev's points, on the other hand, lie inside the range $[-1, 1]$ and are not evenly spaced. To solve this problem, a mapping function was presented, as previously documented by Reddy *et al.* (1999); Juniper *et al.* (2014):

$$y = -\frac{l\tilde{y}}{\sqrt{1 + s - \tilde{y}^2}}, \tag{17}$$

where $l = 0.8, s = (l/s_\infty)^2$, $s_\infty = 25$ and $\tilde{y} \in [-1, 1]$ refers to the Chebyshev points. With this mapping, the domain becomes $y \in [-s_\infty, s_\infty]$. The constant l is the refinement parameter chosen from the tests performed. The numerical code was implemented in the Matlab software, and the eigenvalues and eigenvectors were obtained using the Matlab command `eig`.

3.2 Direct Numerical Simulation

Numerical resolution via Direct Numerical Simulation (DNS) uses techniques for both spatial and temporal discretizations. This study makes the assumption that the flow is periodic in the x direction, which makes it possible to apply a spectral method that makes use of fast Fourier transforms. Meanwhile, a stretched computational mesh was used in the y direction with high-order compact finite difference schemes (Souza, 2003; Souza *et al.*, 2005; Lele, 1992; Kloker, 1997). A classical fourth-order Runge–Kutta integration scheme is used to discretize the time derivatives in the vorticity transport and the components of the non-Newtonian extra-stress tensor equations (Ferziger *et al.*, 2019).

4. RESULTS

The numerical results considered two main longitudinal modes: the varicose (symmetric) and the sinuous (antisymmetric) modes. These are Kelvin-Helmholtz instability modes, which, due to the existence of inflection points in the velocity profile — places where the velocity's curvature changes sign — represent the kind of instability controlling jet flows. The amplification of disturbances caused by these inflection points may result in the formation of vortices and turbulent flow patterns.

Using the Linear Stability Theory approach, a temporal analysis was conducted for two specific cases, $Re = 100$, $\beta = 0.7$ and $Wi = 10$, and $Re = 500, \beta = 0.1$ and $Wi = 5$. The Newtonian result was used for comparison in both cases. The temporal growth rate for the sinuous and varicose modes is displayed in Figures 1 and 2, respectively. For these results, we used the Newtonian fluid and the Oldroyd-B and Giesekus models with $\alpha_G = 0.1, 0.3$, and 0.5.

The range of unstable wave number is observed to increase with an increase in Reynolds number for the Newtonian case, and the maximum value of the temporal growth rate ω_i is also observed to increase. Giesekus and Oldroyd-B fluids behave similarly, however the unstable wave number range is larger as the mobility parameter α_G increases.

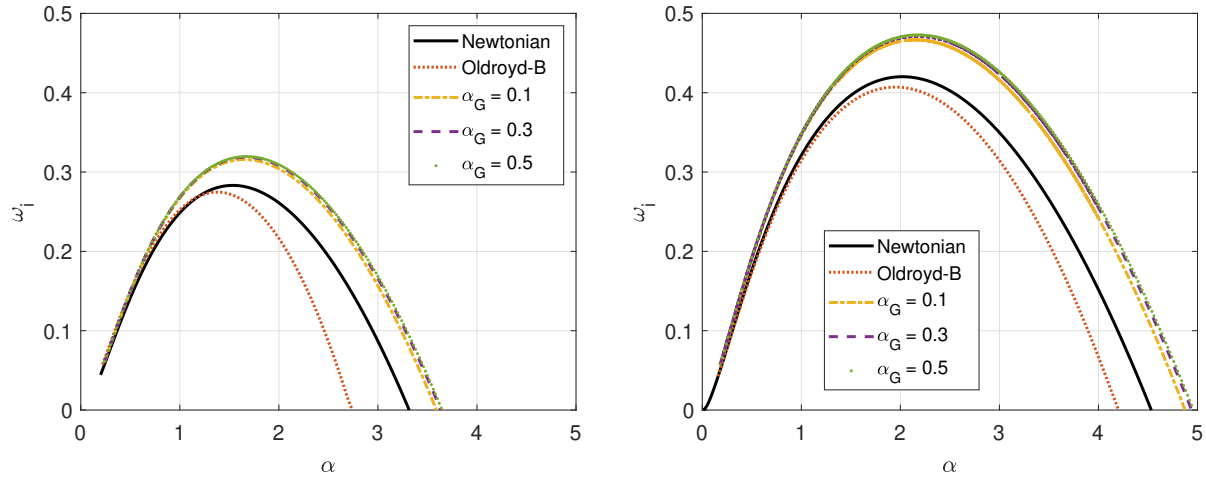

(a) (b)

Figure 1. Temporal growth rate for the sinuous mode: (a) $Re = 100, \beta = 0.7$ and $Wi = 10$ and (b) $Re = 500, \beta = 0.1$ and $Wi = 5$.

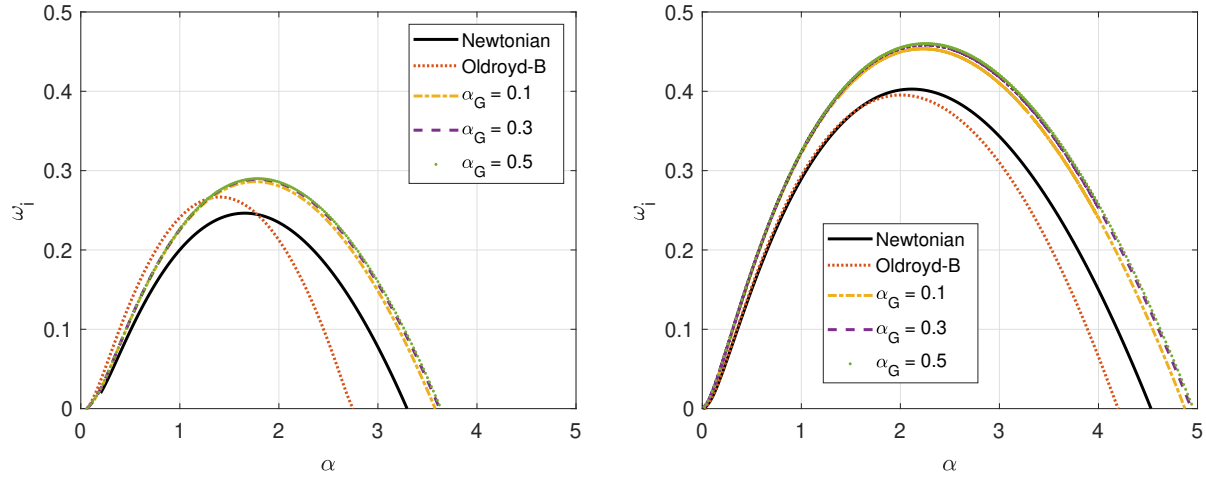

(a) (b)

Figure 2. Temporal growth rate for the varicose mode: (a) $Re = 100, \beta = 0.7$ and $Wi = 10$ and (b) $Re = 500, \beta = 0.1$ and $Wi = 5$.

The data used for the three Direct Numerical Simulations came from the temporal LST study. To validate the code for various dimensionless parameters, two cases of viscoelastic fluid flows (cases B and C) and a Newtonian fluid flow (case A) were simulated. Table 1 presents the results.

Table 1. Data chosen for Direct Numerical Simulation.

					ω_r			
Case	Re	β	Wi	α	Oldroyd-B	$\alpha_G = 0.1$	$\alpha_G = 0.3$	$\alpha_G = 0.5$
A	100	1	0	1.5	7.1569×10^{-1}	7.1569×10^{-1}	7.1569×10^{-1}	7.1569×10^{-1}
B	100	0.7	10	0.25	3.5444×10^{-2}	2.7356×10^{-2}	2.7561×10^{-2}	2.7659×10^{-2}
C	500	0.1	5	0.2	2.2605×10^{-2}	2.9417×10^{-2}	3.0360×10^{-2}	3.0708×10^{-2}

The variation of the maximum streamwise disturbance amplitude u_{max} in the streamwise direction yields the temporal growth rate ω_i for each case. The outcomes are contrasted with the LST findings, which are shown in Table 2 – 5. Tables 2 and 3 show the comparison of the temporal growth rate for the sinuous mode, while Tables 4 and 5 refer to varicose mode. The comparison with LST results is satisfactory, demonstrating that the study of Newtonian and non-Newtonian fluid flows is consistent with both LST and DNS results.

Table 2. Comparison DNS and LST results for sinuous mode (Oldroyd-B and Giesekus with $\alpha_G = 0.1$).

	Oldroyd-B		$\alpha_G = 0.1$	
Case	ω_{iLST}	ω_{iDNS}	ω_{iLST}	ω_{iDNS}
A	2.8305×10^{-1}	2.8304×10^{-1}	2.8305×10^{-1}	2.8304×10^{-1}
B	6.7809×10^{-2}	6.7809×10^{-2}	6.42576×10^{-2}	6.42579×10^{-2}
C	5.7691×10^{-2}	5.7692×10^{-2}	6.5039×10^{-2}	6.5040×10^{-2}

Table 3. Comparison DNS and LST results for sinuous mode (Giesekus with $\alpha_G = 0.3$ and 0.5).

	$\alpha_G = 0.3$		$\alpha_G = 0.5$	
Case	ω_{iLST}	ω_{iDNS}	ω_{iLST}	ω_{iDNS}
A	2.8305×10^{-1}	2.8304×10^{-1}	2.8305×10^{-1}	2.8304×10^{-1}
B	6.4520×10^{-2}	6.4520×10^{-2}	6.4645×10^{-2}	6.4644×10^{-2}
C	6.5824×10^{-2}	6.5824×10^{-2}	6.6143×10^{-2}	6.6144×10^{-2}

Table 4. Comparison DNS and LST results for varicose mode (Oldroyd-B and Giesekus with $\alpha_G = 0.1$).

	Oldroyd-B		$\alpha_G = 0.1$	
Case	ω_{iLST}	ω_{iDNS}	ω_{iLST}	ω_{iDNS}
A	2.4386×10^{-1}	2.4400×10^{-1}	2.4386×10^{-1}	2.4400×10^{-1}
B	5.1883×10^{-2}	5.1728×10^{-2}	3.7985×10^{-2}	3.7892×10^{-2}
C	4.5328×10^{-2}	4.5253×10^{-2}	5.6174×10^{-2}	5.6176×10^{-2}

Table 5. Comparison DNS and LST results for varicose mode (Giesekus with $\alpha_G = 0.3$ and 0.5).

	$\alpha_G = 0.3$		$\alpha_G = 0.5$	
Case	ω_{iLST}	ω_{iDNS}	ω_{iLST}	ω_{iDNS}
A	2.4386×10^{-1}	2.4400×10^{-1}	2.4386×10^{-1}	2.4400×10^{-1}
B	3.8310×10^{-2}	3.8333×10^{-2}	3.8475×10^{-2}	3.8579×10^{-2}
C	5.7445×10^{-2}	5.7471×10^{-2}	5.7952×10^{-2}	5.7984×10^{-2}

The outcomes of the two methods can be observed to be in good agreement, with the sinuous mode displaying slightly greater accuracy than the varicose mode.

5. CONCLUSIONS

The presented results indicate that studying the behavior of Newtonian and non-Newtonian fluids subject to Kelvin-Helmholtz instabilities in jet flows can be effectively accomplished through the use of the Linear Stability Theory (LST)

and Direct Numerical Simulations (DNS) approaches. For both Newtonian fluids and the Oldroyd-B and Giesekus viscoelastic models, we found that as the Reynolds number increased, the range of unstable frequencies and the maximum temporal growth rate increased when examining the varicose and sinuous modes.

The consistency between the two approaches was demonstrated when the outcomes of the numerical simulations were successfully verified against data collected by LST. The meandering mode yielded the most satisfactory agreement between the two approaches, while the varicose mode also produced robust results.

6. ACKNOWLEDGEMENTS

The authors thank the *Coordenação de Aperfeiçoamento de Pessoal de Nível Superior* (CAPES) for the research grant received during the development of this study. The research was carried out using the computational resources of the Center for Mathematical Sciences Applied to Industry (CeMEAI), funded by FAPESP (grant 2013/07375-0).

7. REFERENCES

Brandi, A.C., Gervazoni, E.S., Mendonça, M.T. and Souza, L.F., 2017. "Investigação da estabilidade em escoamento bidimensional para o fluido Oldroyd-B". In *Proceeding Series of the Brazilian Society of Computational and Applied Mathematics*. São José dos Campos, Brasil.

Brandi, A.C., Mendonça, M.T. and Souza, L.F., 2019. "DNS and LST stability analysis of Oldroyd-B fluid in a flow between two parallel plates". *Journal of Non-Newtonian Fluid Mechanics*, Vol. 267, pp. 14 – 27. ISSN 0377-0257. doi:10.1016/j.jnnfm.2019.03.003.

Ferziger, J.H., Perić, M. and Street, R.L., 2019. *Computational methods for fluid dynamics*. springer.

Furlan, L.J., Brandi, A.C., Mendonça, M.T., Silva, A.A. and Souza, M.T.A.L.F., 2018. "Lst of oldroyd-b and giesekus fluids flow stability". In *ABCM Spring School on Transition and Turbulence - EPTT*. ABCM.

Guimarães, M.C., Pinho, F.T. and da Silva, C.B., 2023. "Viscoelastic jet instabilities studied by direct numerical simulations". *Phys. Rev. Fluids*, Vol. 8, p. 103301. doi:10.1103/PhysRevFluids.8.103301.

Guimarães, M.C., Pimentel, N., Pinho, F.T. and da Silva, C.B., 2020. "Direct numerical simulations of turbulent viscoelastic jets". *Journal of Fluid Mechanics*, Vol. 899, p. A11. doi:10.1017/jfm.2020.402.

Juniper, M.P., Hanifi, A. and Theofilis, V., 2014. "Modal Stability Theory: Lecture notes from the FLOW-NORDITA Summer School on Advanced Instability Methods for Complex Flows, Stockholm, Sweden, 2013". *Applied Mechanics Reviews*, Vol. 66, No. 2. ISSN 0003-6900. doi:10.1115/1.4026604. 024804.

Kloker, M.J., 1997. "A robust high-resolution split-type compact FD scheme for spatial direct numerical simulation of boundary-layer transition". *Applied scientific research*, Vol. 59, pp. 353–377.

Kundu, P. and Cohen, I., 2010. *Fluid Mechanics*. Academic Press, Kidlington, 4th edition.

Lele, S.K., 1992. "Compact finite difference schemes with spectral-like resolution". *Journal of Computational Physics*, Vol. 103, No. 1, pp. 16–42. ISSN 0021-9991. doi:https://doi.org/10.1016/0021-9991(92)90324-R.

Michalke, A., 1971. *Instabilität eines kompressiblen runden Freistrahls unter Berücksichtigung des Einflusses der Strahlgrenzschichtdicke*, Vol. 19. English Translation: 1977, NASA Technical Memorandum 75190.

Rallison, J.M. and Hinch, E.J., 1995. "Instability of a high-speed submerged elastic jet". *J. Fluid Mech*, pp. 311–324.

Reddy, S.C., Weideman, J.A.C. and Norris, G.F., 1999. "On a modified Chebyshev pseudospectral method". *Report, Oregon State University*.

Souza, L.F., 2003. *Instabilidade centrífuga e transição para turbulência em escoamentos laminares sobre superfícies côncavas*. Ph.D. thesis, Instituto Tecnológico de Aeronáutica.

Souza, L.F., Mendonça, M.T. and Medeiros, M.A.F., 2005. "The advantages of using high-order finite differences schemes in laminar–turbulent transition studies". *International Journal for Numerical Methods in Fluids*, Vol. 48, No. 5, pp. 565–582. doi:https://doi.org/10.1002/fld.955.

Sterza, R.L., de Mendonca, M.T., de Souza, L.F. and Brandi, A.C., 2023a. "Investigation of the stability of a planar Oldroyd-B jet". *Journal of the Brazilian Society of Mechanical Sciences and Engineering*, Vol. 45. doi:10.1007/s40430-023-04162-5.

Sterza, R.L., de Souza, L.F., Cavalieri, A., de Mendonca, M.T. and Brandi, A.C., 2023b. "Stability analysis of oldroyd-b and giesekus fluids in a planar jet flow". In *Proceedings of the 27th International Congress of Mechanical Engineering*. ABCM. doi:10.26678/ABCM.COBEM2023.COB2023-1843.

Sterza, R.L., de Souza, L.F., de Mendonca, M.T. and Brandi, A.C., 2022. "Shooting and matrix method applied to the analysis of stability of viscoelastic jet flows". In *Proceedings of the 13th Spring School on Transition and Turbulence*. ABCM, EPTT22. doi:10.26678/abcm.eptt2022.ept22-0018.

Zhang, M., 2012. *Linear stability analysis of viscoelastic flows*. Master's thesis, Royal Institute of Technology.

Zhang, M., Lashgari, I., Zaki, T.A. and Brandt, L., 2013. "Linear stability analysis of channel flow of viscoelastic Oldroyd-B and FENE-P fluids". *Journal of Fluid Mechanics*, Vol. **737**.

8. RESPONSIBILITY NOTICE

The authors are the only responsible for the printed material included in this paper.